Water **2014**, *6*, 584-601; doi:10.3390/w6030584

OPEN ACCESS

water

ISSN 2073-4441
www.mdpi.com/journal/water

Article

Submarine Groundwater Discharge at a Single Spot Location: Evaluation of Different Detection Approaches

Michael Schubert [1,*], Jan Scholten [2], Axel Schmidt [3], Jean François Comanducci [4], Mai Khanh Pham [4], Ulf Mallast [1] and Kay Knoeller [1]

[1] Helmholtz-Centre for Environmental Research–UFZ, Leipzig 04318, Germany; E-Mails: ulf.mallast@ufz.de (U.M.); kay.knoeller@ufz.de (K.K.)
[2] Institute of Geosciences, University Kiel, Kiel 24118, Germany; E-Mail: js@gpi.uni-kiel.de
[3] German Federal Institute of Hydrology, Koblenz 56068, Germany; Helmholtz-Centre for Environmental Research–UFZ, Leipzig 04318, Germany; E-Mail: Axel.Schmidt@bafg.de
[4] International Atomic Energy Agency (IAEA)–Environment Laboratories, 98000 Monaco; E-Mails: J.Comanducci@iaea.org (J.F.C.); M.Pham@iaea.org (M.K.P.)

* Author to whom correspondence should be addressed; E-Mail: michael.schubert@ufz.de; Tel.: +49-341-235-1410; Fax: +49-341-235-1443.

Received: 6 December 2013; in revised form: 28 February 2014 / Accepted: 4 March 2014 / Published: 24 March 2014

Abstract: Submarine groundwater discharge (SGD) into the ocean is of general interest because it acts as vehicle for the transport of dissolved contaminants and/or nutrients into the coastal sea and because it may be accompanied by the loss of significant volumes of freshwater. Due to the large-scale and long-term nature of the related hydrological processes, environmental tracers are required for SGD investigation. The water parameters of electrical conductivity and temperature, the naturally occurring radionuclides of radon and radium as well as the stable water isotopes ^{18}O and ^{2}H have proven in previous studies their general suitability for the detection and quantification of SGD. However, individual hydrogeological settings require a site-specific application of this "tool box". This study evaluates and compares the applicability of the abovementioned tracers for investigating SGD from a distinct submarine source in a karst environment at Cabbé, southern France. The specific advantages and disadvantages of each individual parameter under the given hydrogeological conditions are discussed. Radon appeared to be the most suitable environmental tracer in the site specific context. The water temperature was less reliable due to the little temperature difference between seawater and groundwater and since the diurnal variation of the air temperature masks potential SGD signals. Radium isotopes are less

applicable in the studied region due to the lack of a well-developed subterranean estuary. The stable water isotopes showed results consistent with the salinity and radon data; however, the significantly higher effort required for stable isotope analyses is disadvantageous. A multi-temporal thermal remote sensing approach proved to be a powerful tool for initial SGD surveying.

Keywords: submarine groundwater discharge; SGD; environmental tracers; radon; radium; stable isotopes; multi-temporal thermal remote sensing

1. Introduction

Along the coastlines worldwide, terrestrial waters discharge continuously into the coastal sea. A key role in the related water budget is played by submarine groundwater discharge (SGD), *i.e.*, "the flow of water through the continental margin from the seabed to the coastal ocean, occurring regardless of fluid composition or driving force with scale lengths of meters to kilometres" [1].

Due to two general facts SGD is of major interest for coastal water resources management: (1) it provides transport for contaminants and/or nutrients, thereby potentially threatening marine ecosystem health; (2) it may cause a loss of substantial volumes of freshwater to the ocean. With regard to the first, several studies have shown that dissolved material transport associated with SGD can be of the same order of magnitude as material transport associated with river discharge and surface water runoff [2,3]. With regard to the second it can be stated, that particularly spots of focussed SGD have the so far unexploited potential to be used as important freshwater sources in arid climate zones and/or other areas that are characterized by water scarcity (e.g., islands in the Mediterranean Sea). The overall water resources management context of SGD is not only of relevance in the coastal ocean but also linked to the phenomenon offshore fresh groundwater reserves as comprehensively discussed by Post *et al.* [4].

In comparison to the investigation of river water discharge into the sea, which allows straightforward quantification of discharge rates and material budgets, the localization and investigation of SGD is more complex. Besides the difficulty that SGD can occur as both, diffuse seeps across wide patches of sea floor and focussed flow emerging from a distinct submarine spring, it is the high temporal variability that complicates the localisation of SGD areas and the assessment of the associated environmental impacts. The main drivers causing temporal fluctuations in SGD are (1) seasonal and long-term, changes in the inland hydraulic head; (2) tidal-driven, *i.e.*, diurnal changes in pressure gradients; and (3) short-term non-cyclical wave or current-induced pressure gradients [5].

A considerable number of scientific studies during the last two decades have investigated occurrences of SGD in different environmental settings [3,6–14]. These studies revealed that in-depth understanding of SGD and related processes demands approaches that apply environmental tracers, *i.e.*, naturally-occurring hydrochemical indicators or dissolved tracers that show substantial gradients at the groundwater/seawater interface.

Indicators that are frequently used in this regard include the water parameters specific electrical conductivity (EC)/salinity and the naturally-occurring radioactive noble gas radon. The two parameters show the advantage of straightforward on-site detectability [10,15]. The radionuclide radon-222

(^{222}Rn, hereinafter referred to as radon) is of particular suitability in the given context, since it is short-lived (half-life 3.82 d) and chemically inert, which makes it a preferable dissolved tracer in the field of hydrological sciences [13,16–20].

Besides the two on-site detectable parameters EC and radon, the four naturally-occurring radium isotopes ^{226}Ra, ^{228}Ra, ^{223}Ra, and ^{224}Ra are widely used as environmental tracers for the investigation of groundwater/seawater water interaction and coastal water mixing [21,22]. While radium is mainly particle-bound in freshwater (*i.e.*, not in solution), it desorbs from the mineral matrix if the groundwater salinity rises as is the case in the mixing zone between seawater and freshwater, the so-called "subterranean estuary" [23]. Because the four radium isotopes cover a wide range of half-lives (^{223}Ra: $t_{1/2}$ = 11.4 days; ^{224}Ra: $t_{1/2}$ = 3.7 days; ^{228}Ra: $t_{1/2}$ = 5.75 years; ^{226}Ra: $t_{1/2}$ = 1600 years) mixing processes of discharging groundwater with seawater can be investigated on different spatial and temporal scales.

Also suitable as SGD indicators are the isotopic signatures of δ^{18}O and δ^{2}H, which differ in general significantly between groundwater and surface water bodies [24,25]. Both isotopes can be used as tracers for describing mixing ratios between waters masses of different origin [26].

The presented study was carried out at Cabbé within the Bay of Roquebrune close to Monaco (Figure 1). The site is characterized by focussed groundwater discharge from a major karst aquifer at a distinct submarine spring into the Mediterranean Sea. Cabbé was chosen as study site because it represents an archetypal and easily accessible site representative for coastal zones that are dominated by karst aquifers (as in large parts of the northern Mediterranean).

Figure 1. Small-scale site morphology; the white circle highlights the vertical submarine cave structure. Ropes were used for supporting probes and sampling tubes.

In karst environments large portions of the occurring precipitation recharge the local aquifer directly without large temporal delay, which in turn discharges mainly as focussed SGD into the sea. Zektser *et al.* [27] estimated a SGD flux to the Mediterranean Sea of about 68 km³/a, which corresponds to one third of the overall river discharge to the Mediterranean Sea. At the Cote d´Azur, France, between Nice and Menton over 50 sites of focussed SGD have been localized, which, based on local hydrogeological water mass balances, discharge in total about 18.9×10^6 m^3a^{-1} of freshwater to the sea [28]. However, the significance of this focused SGD for chemical input to the coastal sea remains so far unclear.

The objective of this study was to evaluate and compare the informative value of the abovementioned parameters under the specific conditions of a typically focussed SGD from a submarine karst spring. The investigated tracers included the stable isotopes of water (^{2}H and ^{18}O), naturally-occurring radioactive isotopes (^{222}Rn, $^{228, 226, 224, 223}Ra$) as well as physical (temperature) and chemical water parameters (salinity). Temporal and spatial patterns of all tracers were recorded over a 24 h period at Cabbé and along a 1.75 km transect located within the Bay of Roquebrune. In addition, the applicability of a multi-temporal thermal remote sensing approach [29] was evaluated for supporting the tracer results (and *vice versa*).

2. Methods

2.1. Site Setting

The submarine spring Cabbé is located in the north-western Mediterranean Sea about 5 km NE of Monaco (Figure 2). It is part of a group of several submarine springs mainly occurring along the coast between Nice and Menton, southern France [30]. At Cabbé groundwater discharges in a water depth of about 4 m from the base of a vertical submarine cave with a diameter of approximately 3 m (Figure 1). The cave is surrounded by limestone forming a vertical hole that is constantly inundated by seawater. It is hydraulically connected to a major karst aquifer. Groundwater residence times in this karst aquifer were estimated to be between eight to nine days [30] (*cf.* Section 3.1.6). The yearly average temperature in the region is ~15 °C with an average of 770 mm of precipitation.

Figure 2. Regional setting of the site and the measured transect (**A**) within the Mediterranean Sea; (**B**) in geographical relation to Monaco.

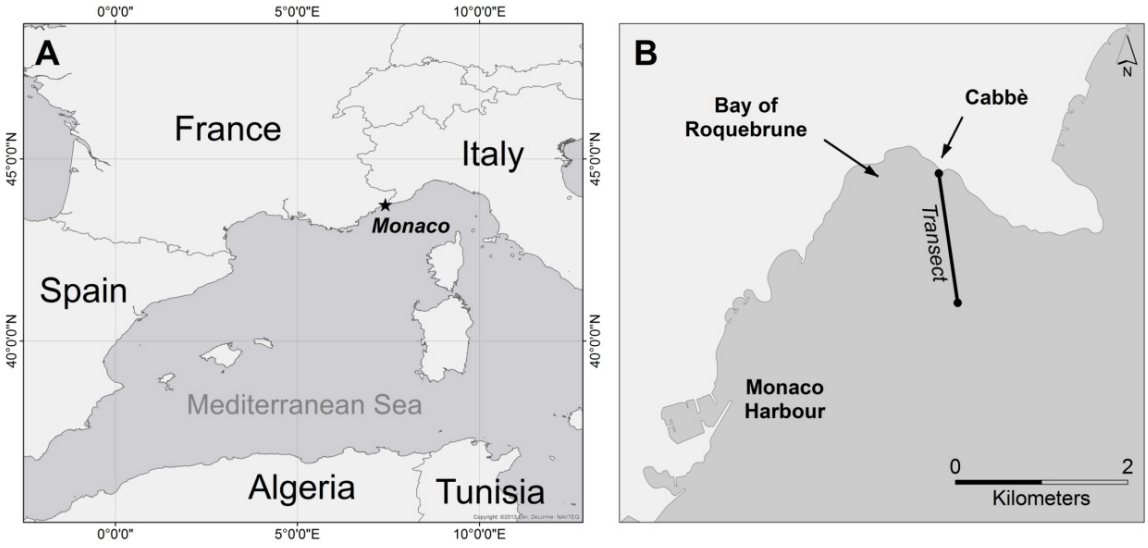

Geologically the area is part of the SE front of a subalpine range called "Arc de Nice", which consists of a series of south-verging folds and thrusts involving Mesozoic and Palaeogene sediments. The sediments consist of marls, clays, dolomites and limestones. Important aquifers with deep karstic circulation are associated with the latter. Coastal and submarine groundwater discharge spots are generally situated at the contact between the Jurassic limestone and the Cretaceous marls and clays.

2.2. Materials and Methods

At the base of the submarine vertical cave, *i.e.*, at the submarine spring, the parameters temperature, salinity, radon concentration, and water depth were monitored using automated detection equipment. All instruments were working properly from about 16:00 on the first day of the 24 h monitoring campaign and measured continuously for 24 h. A recording gap occurred on the second day between 03:00 and 05:00 due to technical difficulties. In addition to the recording of 24 h time series, discrete water samples were taken every 60 min for stable isotope analyses. Four discrete samples for radium analyses were obtained on the second day covering a period between low and high tide.

Additionally to the time-series measurements at the submarine spring, a survey was undertaken along a 1750 m transect within the Bay of Roquebrune starting at the submarine cave Cabbé. Along the transect the parameters salinity, temperature and radon concentration were monitored continuously while cruising with a speed of about 5 km/h. For stable isotopes and radium measurements discrete samples were taken along the transect.

For the measurement of conductivity/salinity, temperature, and water depth a CTD probe (YSI Inc., Yellow Springs, OH, USA) was used. At the spring the CTD was lowered into the cave with ropes (*cf*. Figure 1) and fixed close to the bottom of the vertical cave structure. The recorded water depth was used for monitoring the tidal cycle and for assessing the water turbulence within the cave (wave intensity). Along the transect the CTD was dragged behind the boat in a water depth of about 2 m for temperature and salinity recording. All CTD data were recorded in 10 second intervals. For comparison with the other monitored parameters, suitable moving average values were calculated.

For measurement of radon-in-water concentrations the portable radon-in-air monitor RAD-7 (Durridge Company, Billerica, MA, USA) was used. For radon detection, water was pumped either from the surface sea water (transect) or from the bottom part of the submarine cave. Radon was extracted from the constant water stream into a closed air loop by means of a RAD-Aqua extraction-module as described in detail by e.g., Schmidt *et al.* [15]. In order to achieve radon measurements with uncertainties of about ±10% two RAD-7s were run in parallel with a 30 min counting cycle (30 min time interval between actual readings). The radon concentration that was measured in the air loop was converted into the related radon-in-water concentration by applying the temperature and salinity dependent water/air partition coefficient $K_{a/w}$ of radon [31]. Thus a continuous time series with 30 min detection intervals was achieved.

For the analysis of radium concentrations ($^{223, 224, 226, 228}$Ra), 70 litres of water were pumped either from the bottom part of the submarine cave or from surface sea water (~2m water depth) along the transect. The water was pumped over MnO_2-fibre cartridges with a pump rate of about 1 l/min in order to scavenge the radium quantitatively [8]. The short-lived ^{223}Ra and ^{224}Ra were measured using the RaDeCC delayed coincidence counting system [32] following the procedure described in Moore [8] and Scholten *et al.* [33]. For the long-lived ^{226}Ra and ^{228}Ra measurements the MnO_2-fibres were ashed and prepared for gamma spectrometry measurements [21].

Sampling for stable water isotopes (^{2}H and ^{18}O) was carried out every 60 min from the bottom part of the submarine spring. Along the transect five discrete samples were taken at equidistant locations. All stable isotope samples were collected in 30 mL HDPE bottles and were measured using a continuous flow high temperature pyrolysis unit combined with an isotope ratio mass spectrometer

(IRMS) delta plus XL Thermo Finnigan [34]. The isotopic composition of all samples was determined by the H_2O-H_2 equilibration method (for ^2H) with an analytical precision of ±1.0‰ and the H_2O-CO_2 equilibration method (for ^{18}O) with an analytical precision of ±0.1‰. The results of the hydrogen and oxygen isotope measurements are expressed as delta notations (δ^2H, $\delta^{18}O$) relative to the Vienna Standard Mean Ocean Water (VSMOW).

The applied multi-temporal thermal remote sensing approach was based on eight Landsat ETM+ band 6.2 (high gain) images (path 194/row 30). All images were recorded during the hydrological summer (May-October) of the years 2000–2009 at 12:00 a.m. local time (GMT+2). Each image, which exhibits a ground sampling distance (GSD) of 30 m, was co-registered to UTM WGS 84 Zone 32N. For images recorded after the 31 May 2003, the gaps caused by SLC (scan line corrector) failure of Landsat were filled using the triangulation method implemented in the Envi 4.7 software package. Further data processing included the conversion from digital numbers to sea-surface temperatures (SST) including an atmospheric correction of each image. The applied value for water emissivity is 0.98. Values for atmospheric transmissivity, upwelling and downwelling radiances needed for the atmospheric correction of each image were obtained through the web-based Atmospheric Correction Tool that is based on MODTRAN [35]. The identification of SGD locations was based on the assumption that temperatures of discharging groundwater are less variable than ambient seawater temperatures. Hence the standard deviation of the temperature per pixel of the SST-image time-series was calculated and used as indicator [29].

3. Results and Discussion

3.1. Cabbé Submarine Spring

3.1.1. Water Turbulence and Tidal Cycle

The water turbulence was recorded because it has a strong impact on the conditions in the vertical cave, namely on (i) the degree of radon degassing from the water; (ii) the intensity of SGD/seawater mixing; and (iii) the temperature of the seawater. In particular at monitoring points that are located close to a rocky shore, as is the case at Cabbé, water turbulence must not necessarily correspond to the actual wind speed since it mainly results from the surf breaking on the rocky shore.

Figure 3 illustrates the wave intensity by showing the short-time deviation of the one minute running average water depth recorded in 10 second steps. With regard to water turbulence the 24 h monitoring period can be divided into two subsections: during the beginning of the sampling campaign, on the first day between 16:00 and 18:00, very turbulent waters were observed. Thereafter, in particular between 12:00 and 16:00 on the second day, the sea became significantly calmer. A data gap between about 03:00–05:00 occurred due to malfunction of the detection equipment.

The recorded water depths were also used for determination of the tidal cycle. The tidal cycle is a major driver for periodic changes in the SGD rate: during low tide the hydraulic gradient between land and sea is higher compared to high tide. This steeper gradient allows more groundwater to discharge from the hydraulically connected aquifer [6]. Figure 4 shows the water depth above the bottom of the submarine cave during the 24 h monitoring campaign.

Figure 3. Wave intensity shown as deviation of the water depth (WL: water depth).

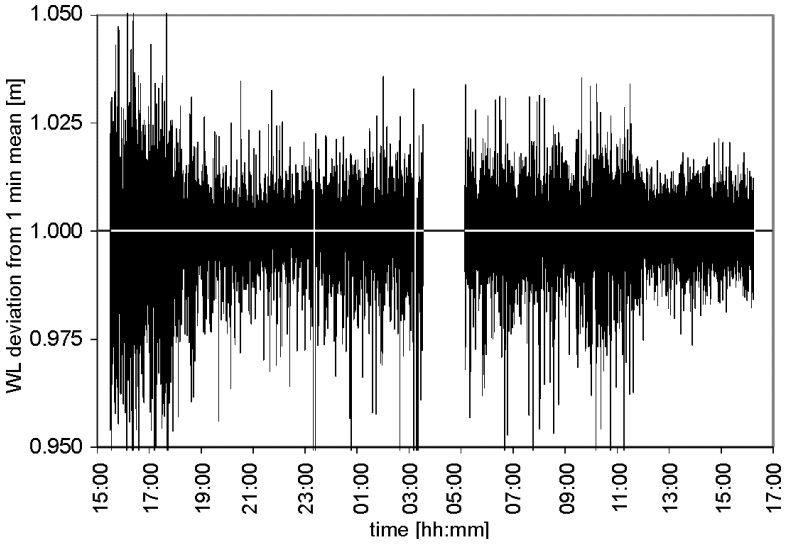

Figure 4. Water column height over the Cabbé submarine spring (*i.e.*, water depth) in 20 min intervals (white diamonds); grey points display individual 10 second readings.

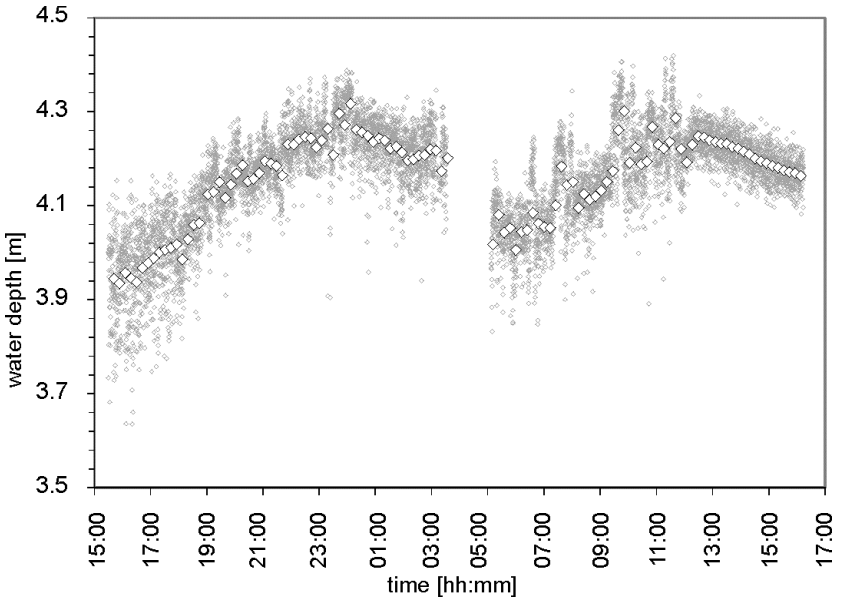

Despite the data gap, tidal periods with low tide at around 16:00 and 04:00 and high tide at around 23:00 and 11:00 can clearly be distinguished. However, even though the data show distinct flood/ebb periods, the water depths recorded during the first four hours (16:00–18:00) were considerably lower than during later ebb stages. That effect is believed to be due to two reasons: (1) strong winds coming off the land at that time pushed water out of the bay resulting in a generally decreased seawater level; (2) the water in the vertical cave, due to the high turbulence (*cf.* Figure 3), was highly enriched with air bubbles reducing the bulk water density and hence the hydrostatic pressure of the water column over the CTD (the CTD applies a pressure transducer for water depth detection). Thus, water depth readings for the period between 16:00 and 18:00 are probably too low. The changing conditions reflected in Figure 3 do affect tracer distribution behavior in the coastal sea in general. Hence the recorded tracer data show a strong dependence on the water turbulence as it will be revealed in the following.

3.1.2. Water Temperature

As illustrated in Figure 5A a distinct positive correlation between temperature and water depth was observed during the second day of the sampling campaign (calm sea). A coefficient of determination of $R^2 = 0.766$ (N = 20) was determined. This relation is caused by the changing hydrostatic pressure on the aquifer correlated to the changing tides. The discharging groundwater has a somewhat lower temperature (~17.5 °C; [30]) than the coastal sea water (~22 °C) thus leading to water temperature decrease in the cave at low tide. However, during the first hours of the campaign (rough sea; low tide) that correlation was seemingly reversed. In spite of the low water depth (and the supposedly associated increased discharge of cool groundwater) the water temperature showed the highest values recorded during the entire campaign. This observation is explained to be as a result of the rough sea (before 18:00, *cf*. Figure 3). The strong surf resulted in a substantial amount of (warm) air bubbles whirling deep in the studied water column, giving rise to a significant increase of the water temperature during that time (the outside air temperature was measured to be around 25 °C that afternoon).

In conclusion it can be stated that whereas in several other studies the water temperature could be applied as a conservative SGD tracer [36], its applicability is limited in regions where the temperature gradient between groundwater and seawater is too small to allow discrimination between diurnal fluctuations of the seawater temperature and water temperature fluctuations caused by SGD. Besides it was shown that water turbulence can have a significant influence on the seawater temperature.

3.1.3. Salinity

As shown in Figure 5B a distinct positive relation between salinity and water depth was observed during the second part of the sampling campaign (calm sea). As expected, high water depths (high tides at 23:00 and 11:00) resulted in increased salinities, an effect that can be attributed to the decreased SGD rate at high tide. However, during the period characterized by rough conditions in the beginning of the campaign (16:00–18:00) this relationship seems to be reversed. In spite of low water depths and related increased SGD rates the recorded salinities were rather comparable to the respective data recorded during the following high tides. It is most likely that the reason for this reversed relationship is the high turbulence of the water during the first hours of monitoring resulting in a more intense exchange of seawater with the discharging groundwater in the submarine cave. Even though the recorded wave heights are maximally 0.1 m, the actual breaking of the waves into the mouth of the cave caused visibly heavy turbulences in the water column of the cave resulting in the recorded inverse trend in salinity (and temperature). Another potential explanation is that seawater, which was pushed into the conduit system earlier during the rough sea conditions, discharged again at low tide after the sea started to calm down.

In terms of its applicability as SGD tracer, salinity can generally be considered more suitable than temperature. Besides the fact that it is not influenced by atmospheric conditions, the salinity gradient at the groundwater/seawater interface is much more distinct than temperature gradients. While off-shore seawaters generally show salinities of around 35 (38.06 in the Bay of Roquebrune) groundwater shows in general negligible or lower salinities (7.2 at Cabbé, see Table 1).

Figure 5. (**A**) Water depth and temperature; (**B**) Salinity; (**C**) Radon concentration; (**D**) Delta ^{2}H; and (**E**) Delta ^{18}O during the 24 h observation period. LT = low tide; HT = high tide.

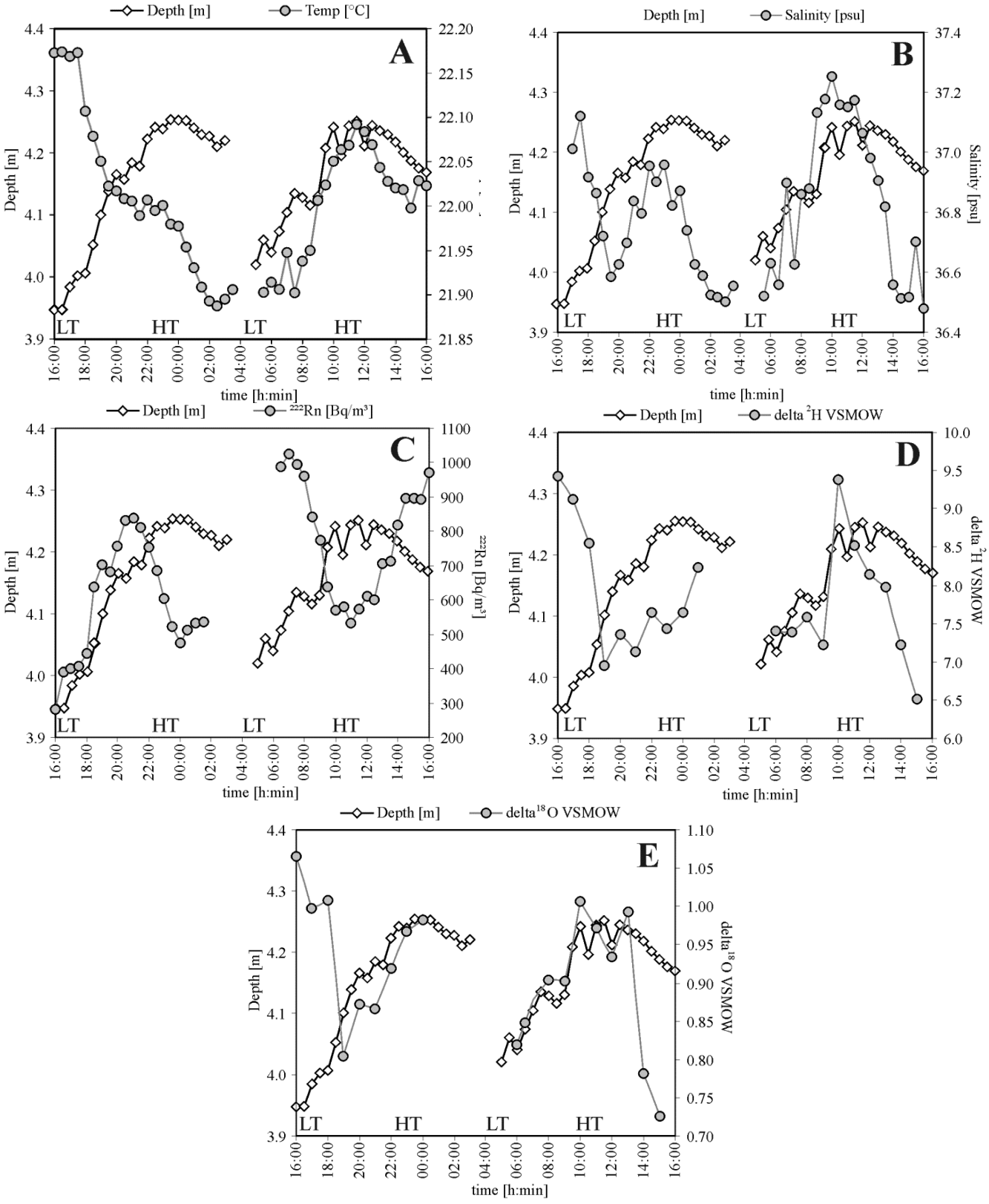

Table 1. Groundwater and off-shore seawater end-members for all applied parameters.

Parameter	Groundwater	Off-shore seawater
salinity	~7.2	38.06
^{222}Rn	28,000 Bq/m^3	<4 Bq/m^3
$\delta^{18}O$	−4.7‰ *	1.22‰
$\delta^{2}H$	−35.1‰ *	10.4‰

Note: * derived from long-term weighted annual mean rain water composition from the local GNIP station in Monte Carlo/Monaco (GNIP station code 769001).

3.1.4. Dissolved Radon Concentrations

Due to the lack of radon production, seawater shows generally a radon background of only a few Bq/m^3. Groundwater concentrations, in contrast, can reach levels of up to 20 kBq/m^3 and more. The strong gradient at the groundwater/seawater interface results in an inverse correlation between seawater depth and radon concentration in the coastal sea, *i.e.*, in high concentrations during low tides (due to intense SGD) and *vice versa* [37].

Figure 5C illustrates the radon data recorded at the base of the submarine cave. As displayed, the expected inverse correlation between radon and water depth was observed from 22:00 until the end of the monitoring campaign (calm sea). For the second day of the campaign a coefficient of determination of $R^2 = 0.624$ (N = 20) was found. At the beginning of the campaign however (rough sea), this relationship appears to be reversed. Low water depths are associated with low radon concentrations in the water column. The most likely reason for this unusual radon pattern is the high water turbulence (as mentioned above). While radon is degassing from every open water surface, this gas evasion is strongly enforced if the water is very turbulent and contains many air bubbles. (The rough sea resulted also in intense water mixing between seawater and discharging groundwater). Radon degassing is due to the water/air partition coefficient of radon which is $K_{w/a} = 0.25$ at the given temperature [31]. Comparable to the interpretation of the salinity data another potential explanation is that seawater, which was pushed into the conduit system earlier, discharged again after the sea started to calm down.

For the applicability of radon as SGD tracer it can hence generally be stated that radon reveals robust data due to its distinct gradient at the groundwater/seawater interface, due to its inert behaviour and due to its straightforward detectability on site. However, in the case of rough seas intense radon degassing may limit its applicability as a tracer.

3.1.5. Dissolved Radium Activity

At Cabbé, radium isotope concentrations do not show clear variations with tides. Also the isotope ratios determined along the transect are in the same range as observed at Cabbé (Figure 6). If SGD at Cabbé were a source of radium one would expect decreasing $^{224}Ra/^{228}Ra$ and/or $^{228}Ra/^{226}Ra$ values with increasing distance from Cabbé.

The lack of radium enrichment in the groundwater discharging at Cabbé is in contrast to several other SGD studies in the Mediterranean Sea where radium has been successfully applied as SGD tracer [38–40]. We explain the lack of radium in the discharging groundwater to be due to two main reasons: (1) The SGD site studied is hydraulically connected to a major karst aquifer. In such oxic

groundwaters radium adsorbs on mineral surfaces and therefore dissolved concentrations are very low. (2) In general radium is released from aquifer mineral surfaces in the mixing zone between seawater and groundwater (subterranean estuary) where increased salinities are present [41]. In contrast to many other settings in the Mediterranean Sea there is no well-developed subterranean estuary at Cabbé. The groundwater discharges directly into the cave without an aquifer zone where radium can be mobilized from the aquifer matrix.

Due to the specific hydrological setting, radium has to be considered less suitable for SGD investigation at Cabbé. This may also be the case for other focused SGD locations having a poorly developed subterranean estuary.

Figure 6. Radium isotope ratios at Cabbé and along the transect. (**A**) $^{224}Ra/^{228}Ra$; (**B**) $^{228}Ra/^{226}Ra$.

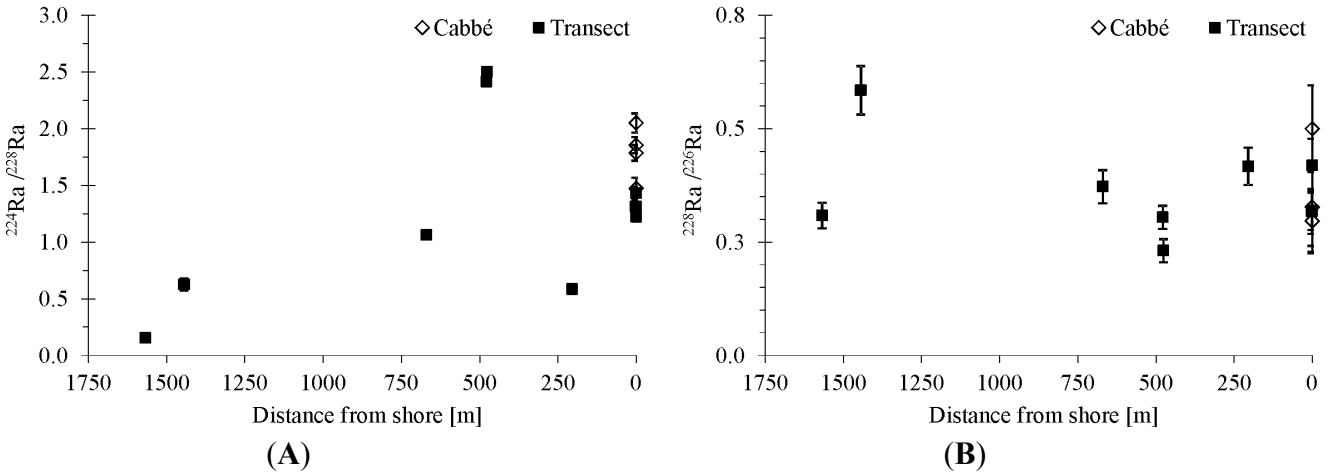

3.1.6. Stable Water Isotopes

As shown in Figure 5D,E the stable isotope signatures of the water show a distinct positive relation with the tides, *i.e.*, the water depth in the submarine cave. Only during the first hours of the observation period a seemingly inverse relationship was found (as already discussed for the other parameters).

The reason for the generally lighter isotopic signatures at low tide is the significant difference in isotopic signatures between seawater and meteoric groundwater. Lighter signatures at low tide indicate increased discharge of isotopically lighter groundwater into the sea. A shift to heavier isotope signatures can be observed at high tides since the water column is less influenced by groundwater at this stage. The inverse behaviour at the beginning of the observation period is most likely caused by intense water mixing between the near-shore seawater and the SGD fed water column in the submarine cave. The strong impacts of the water turbulence and of potentially discharging seawater that was pushed into the conduit system earlier on the stable isotope signatures during the first hours of recording are comparable to the impact on salinity and radon as discussed above.

3.2. Transect

Whereas all parameters recorded at the Cabbé SGD location (submarine spring) were discussed individually as time series, the data recorded along the transect are discussed jointly in the following.

The transect started at a distance of about 50 m from the submarine cave at Cabbé and ended *ca*. 1750 m off-shore in the Bay of Roquebrune. Figure 7 displays the continuously recorded salinity data as 20 min average values. The salinity increases from ~37 at the coastal end of the transect to ~38 at a distance of 600 m off-shore from where it remains constant with increasing distance. Although the absolute gradient is small, it can be seen that SGD has significant influence on a rather large area within the Bay of Roquebrune. It has to be mentioned that no further water influx (surface water, precipitation) occurred during the field campaign, which allows attributing the decreasing salinity solely to the SGD influence.

Figure 7. Water salinity and temperature along the transect.

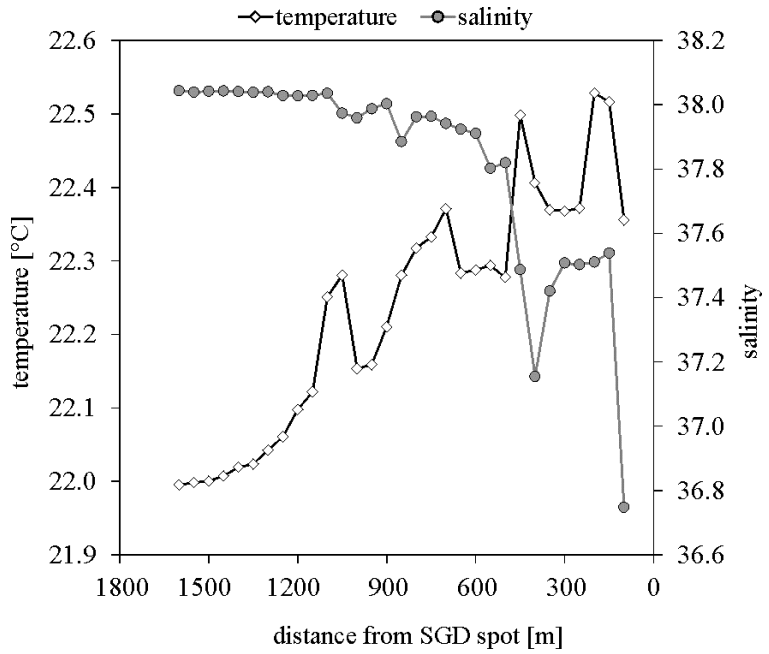

The water temperatures recorded along the transect show a rather indistinct picture with temperatures of about 22.4–22.5 °C close to the shore and later decrease towards the open ocean to a rather constant 22.0 °C. The temperatures measured close to the shore are higher than the highest temperature observed during time-series measurements at Cabbé (maximum temperature 22.0 °C). Thus the temperature variations observed along the transect are most likely not related to SGD at Cabbé. This suggests that temperature is not applicable as a parameter for SGD evaluation at the investigated site.

The stable isotope signatures for $\delta^{18}O$ and $\delta^{2}H$ display a pattern along the transect comparable to salinity (Figure 8). While $\delta^{18}O$ and $\delta^{2}H$ values are constant off-shore both isotopes show a shift to lighter signatures from around 1000 m towards the SGD location. These changes are caused by the discharging groundwater which shows significantly lighter isotopic signatures than the open sea as discussed above.

Radon shows an inverse behaviour as expected. The concentration decreases from 250 Bq/m^3 in the vicinity of the SGD spot, here clearly reflecting the SGD influence, to 4 Bq/m^3 off-shore.

Figure 8. Radon concentrations and water stable isotope signatures along the transect; (**A**) $\delta^{18}O$; (**B**) $\delta^{2}H$.

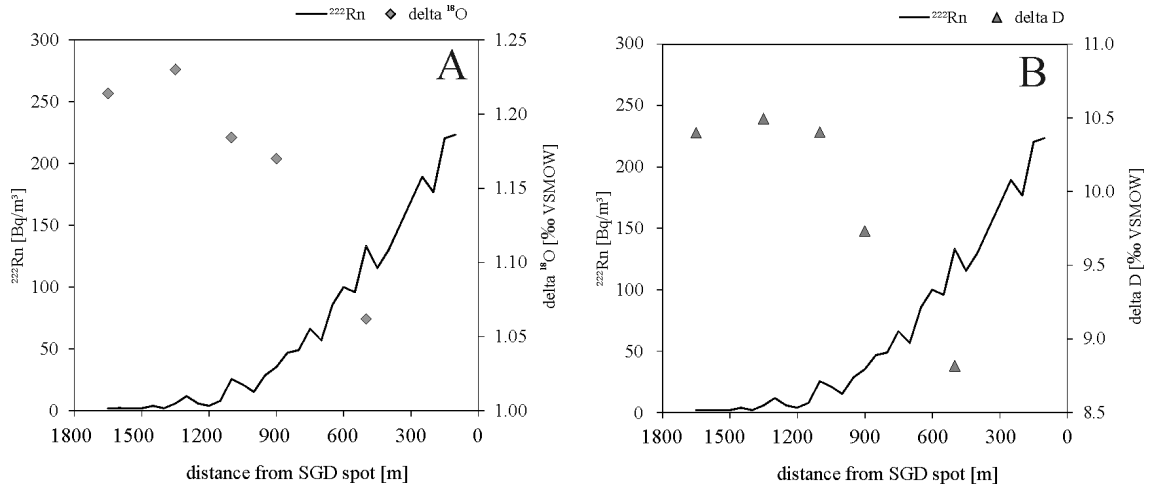

3.3. SST Evaluation

The sea surface temperature (SST) standard deviations within the Bay of Roquebrune are illustrated in Figure 9. The image shows values ranging between 1.8 and 6.0 °C. Areas with high standard deviations indicate varying influence due to e.g., seasonal temperature effects. Areas with low sea-surface temperature variability located close to the shore indicate spatially and thermally persistent groundwater inflow, which stabilizes the seawater temperature in the vicinity of the inflow location.

Figure 9. Sea Surface Temperature ("SST") standard deviation over time within the Bay of Roquebrune (note that small STD values in the proximity of the shore indicate potential Submarine Groundwater Discharge ("SGD") abundance while lower STD values offshore indicate a small SST variability only, caused by the water depth and related high heat capacity of the water column).

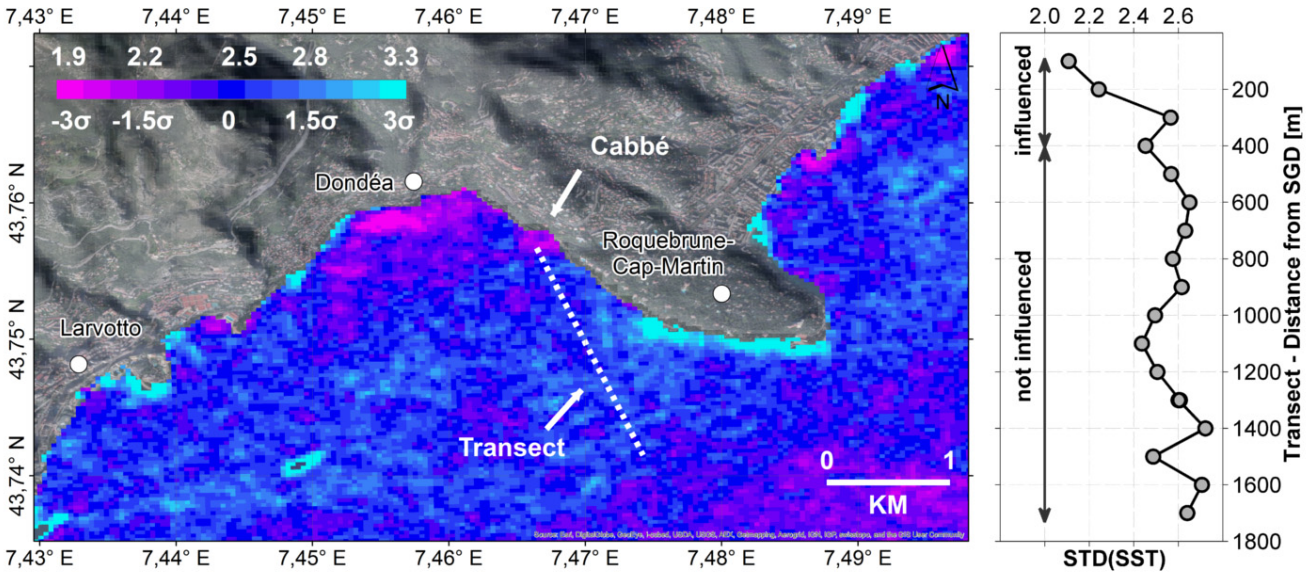

Within the Bay of Roquebrune several areas with small standard deviation values <~2 °C are visible along the coastline. The three most prominent ones are located (i) south of Dondéa; (ii) east of Roquebrune-Cap-Martin at Grimaldi and (iii) at the investigated study site at Cabbé. The latter area has a lateral extent of ~300 m and, unlike the larger area south of Dondéa, no fringe of higher SST standard deviation values in between the actual anomaly and the shoreline. This confirms that groundwater discharges at the shore at Cabbé.

Following the transect from the shore into off-shore direction the SST standard deviation values remain below ~2.3 °C up to a distance of ~200 m from Cabbé. There they increase first abruptly and rise thereafter steadily up to a distance of about 600 m off-shore. The elevated off-shore SST standard deviation values are in accordance with the salinity and radon distribution patterns, which likewise indicate decreasing influence of SGD with increasing distance from Cabbé. Hence it can be stated that, even though the satellite-based approach relies on images recorded long before the actual sampling campaign, the data proves the submarine groundwater discharge at Cabbé to be spatio-temporal constant and provides thus an independent tool for SGD investigation.

3.4. Quantification of Groundwater/Seawater Ratios at Cabbé

A simple two-component mixing equation between end-member concentrations (off-shore water and groundwater) of stable isotopes, radon and salinity was applied for quantifying the relative proportions of groundwater and seawater at Cabbé. For the seawater, end-member values measured at the end of the transect furthest distant from shore were used. Since no groundwater wells were accessible in the immediate vicinity of Cabbé, end-members for radon and salinity were obtained from a well situated directly at the beach at ~500m distance to Cabbé within the same geological/hydrogeological setting. The terrestrial $\delta^{18}O$ and $\delta^{2}H$ end-members were derived from the long-term weighted annual mean rain water composition for the closest GNIP (Global Network of Isotopes in Precipitation) station in Monaco (GNIP station code 769001). The calculation of the annual mean is based on 112 monthly isotope values obtained between 1999 and 2009 [42]. No rain samples were taken in the course of the sampling campaign since no rain had occurred during the study. Table 1 summarizes the end-members for all the parameters used to calculate the percentage of meteoric water in the water column of the Cabbé submarine cave (Figure 10). Generally the results of the SGD indicators give a consistent picture. The fraction of meteoric groundwater in the vertical cave at Cabbé varies between about 1.5%–4.5% for the radon, between 2.0% and 4.0% for the salinity, and between 3.0%–5.0% for the stable isotope data, respectively.

As it can clearly be seen in Figure 10, in particular for the second part of the campaign, the groundwater portion depends on the tidal stage. Generally high tide (HT) periods are characterized by a lower fraction of groundwater in the water column of the vertical cave than low tides (LT). An exception from that generally expected behaviour is the starting period of the campaign, which was characterized by a rough sea influencing tracer distribution behaviour.

Figure 10. Percentage of groundwater in the water in the submarine cave at Cabbé.

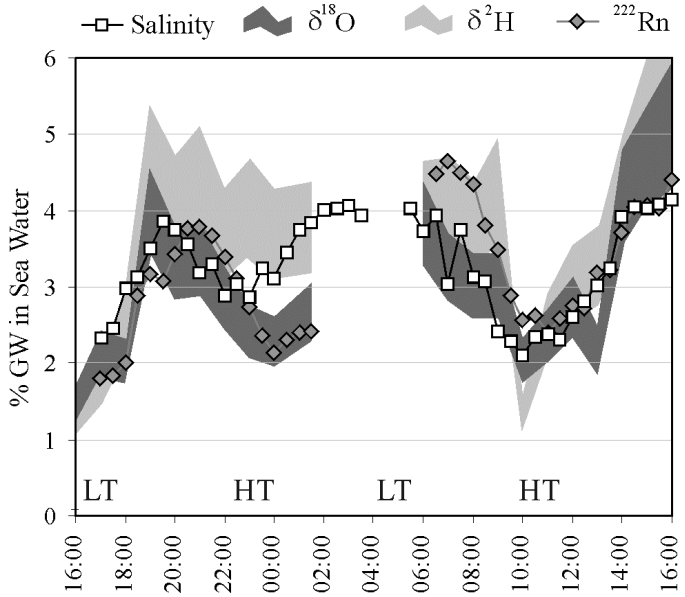

4. Conclusions

We studied the applicability and the informative value of a set of environmental tracers, which have proven in previous studies to be suitable for detecting and quantifying SGD, under the specific conditions of a focussed SGD from a submarine karst spring at Cabbé. Our results show that substantial qualitative and semi-quantitative information can be achieved by applying the easily on-site detectable parameters salinity and radon concentration (^{222}Rn). Radon can be considered as the most robust environmental tracer for SGD in the given case even though radon degassing from the water column has to be considered particularly with rough seas. The temperature of the water column can only be applied as a reliable SGD indicator if the temperature gradient between groundwater and seawater is sufficiently distinct. If it is too small as in the studied case, the diurnal variation of the air temperature masks the potential SGD signals. In our study the naturally-occurring radium isotopes ($^{228, 226, 224, 223}$Ra), were not suitable for detecting SGD, which is interpreted to be due to a poorly developed subterranean estuary inhibiting significant radium mobilization from the aquifer matrix. The stable isotopes of water (^{2}H and ^{18}O) are suitable SGD indicators. In a mass balance approach, stable isotopes, radon and salinity give comparable estimates of the groundwater fraction discharging at Cabbé. The disadvantage of using stable isotopes in comparison to salinity and radon is the significantly higher analytical effort required for stable isotope analyses. Additionally our study showed that a multi-temporal thermal remote sensing approach applying sea surface temperature (SST) patterns can be used as a powerful tool for backing up tracer results and, more importantly as a SGD pre-screening method in order to optimize on-site surveys. Further research is recommended to evaluate the applied "SGD tool box" for the investigation of offshore fresh groundwater reserves.

Conflicts of Interest

The authors declare no conflict of interest.

References

1. Moore, W.S. The effect of submarine groundwater discharge on the ocean. *Annu. Rev. Mar. Sci.* **2010**, *2*, 59–88.
2. Slomp, C.P.; van Cappellen, P. Nutrient inputs to the coastal ocean through submarine groundwater discharge: Controls and potential impact. *J. Hydrol.* **2004**, *295*, 64–86.
3. Santos, I.R.; Niencheski, F.; Burnett, W.; Peterson, R.; Chanton, J.; Andrade, L.C.; Milani, I.; Schmidt, A.; Knoeller, K. Tracing anthropogenic-driven groundwater discharge into a coastal lagoon from southern Brazil. *J. Hydrol.* **2008**, *353*, 275–293.
4. Post, V.E.A.; Groen, J.; Kooi, H.; Person, M.; Shemin Ge, S.; Edmunds, W.M. Offshore fresh groundwater reserves as a global phenomenon. *Nature* **2013**, 504, 71–78.
5. Santos, I.R.; Eyre, B.D.; Huettel, M. The driving forces of pore water and groundwater flow in permeable coastal sediments: A review. *Estuar. Coast. Shelf Sci.* **2012**, *98*, 1–15.
6. Santos, I.R.; Burnett, W.C.; Dittmar, T.; Suryaputra, I.; Chanton, J. Tidal pumping drives nutrient and dissolved organic matter dynamics in a Gulf of Mexico subterranean estuary. *Geochim. Cosmochim. Acta* **2009**, *73*, 1325–1339.
7. Peterson, R.N.; Burnett, W.C.; Taniguchi, M.; Chen, J.Y.; Santos, I.R.; Ishitobi, T. Radon and radium isotope assessment of submarine groundwater discharge in the Yellow River delta, China. *J. Geophys. Res. Oceans* **2008**, *113*, 1978–2012.
8. Moore, W.S. Fifteen years' experience in measuring ^{224}Ra and ^{223}Ra by delayed-coincidence counting. *Mar. Chem.* **2008**, *109*, 188–197.
9. Taniguchi, M.; Iwakawa, H. Submarine groundwater discharge in Osaka Bay, Japan. *Limnology* **2004**, *5*, 25–32.
10. Burnett, W.C.; Dulaiova, H. Estimating the dynamics of groundwater input into the coastal zone via continuous radon-222 measurements. *J. Environ. Radioact.* **2003**, *69*, 21–35.
11. Taniguchi, M. Tidal effects on submarine groundwater discharge into the ocean. *Geophys. Res. Lett.* **2002**, *29*, doi:10.1029/2002GL014987.
12. Corbett, D.R.; Dillon, K.; Burnett, W.C.; Chanton, J.P. Estimating the groundwater contribution into Florida Bay via natural tracers ^{222}Rn and CH_4. *Limnol. Oceanogr.* **2000**, *45*, 1546–1557.
13. Corbett, D.R.; Burnett, W.C.; Cable, P.H.; Clark, S.B. Radon tracing of groundwater input into Par Pond, Savannah River Site. *J. Hydrol.* **1997**, *203*, 209–227.
14. Lee, D.R. A device for measuring seepage flux in lakes and estuaries. *Limnol. Oceanogr.* **1977**, *22*, 140–147.
15. Schmidt, A.; Schlueter, M.; Melles, M.; Schubert, M. Continuous and discrete on-site detection of radon-222 in ground- and surface waters by means of an extraction module. *Appl. Radiat. Isotopes* **2008**, *66*, 1939–1944.
16. Schubert, M.; Brüggemann, L.; Schirmer, M.; Knoeller, K. Radon monitoring in wells as tool for the estimation of the groundwater flow rate. *Water Resourc. Res.* **2011**, *47*, doi:10.1029/2010WR009572.
17. Schmidt, A.; Gibson, J.J.; Santos, I.R.; Schubert, M.; Tattrie, K.; Weiss, H. The relevance of groundwater discharge to the overall water budget of two typical Boreal lakes in Alberta/Canada estimated from a radon mass balance. *Hydrol. Earth Syst. Sci.* **2010**, *14*, 79–89.

18. Schubert, M.; Schmidt, A.; Lopez, A.; Balcázar, M.; Paschkel, A. In-situ determination of radon in surface water bodies by means of a hydrophobic membrane tubing. *Radiat. Measur.* **2008**, *43*, 111–120.
19. Schubert, M.; Bürkin, W.; Peña, P.; Lopez, A.; Balcázar, M. On-site determination of the radon concentration in water samples: Methodical background and results from laboratory studies and a field-scale test. *Radiat. Measur.* **2006**, *41*, 492–497.
20. Schubert, M.; Paschke, A.; Bednorz, D.; Bürkin, W.; Stieglitz, T. The kinetics of the water/air phase transition of radon and its implication on detection of radon-in-water concentrations: Practical assessment of different on-site radon extraction methods. *Environ. Sci. Technol.* **2012**, *46*, 8945–8951.
21. Charette, M.A.; Buesseler, K.O.; Andrews, J.E. Utility of radium isotopes for evaluating the input and transport of groundwater-derived nitrogen to a Cape Cod estuary. *Limnol. Oceanogr.* **2001**, *46*, 465–470.
22. Charette, M.A.; Moore, W.S.; Burnett, W.C. Uranium- and Thorium-Series Nuclides as Tracers of Submarine Groundwater Discharge. In *Radioactivity in the Environment*; Krishnaswami, S., Cochran, J.K., Eds.; Elsevier: Oxford, UK, 2008.
23. Moore, W.S. The subterranean estuary: A reaction zone of ground water and sea water. *Mar. Chem.* **1999**, *65*, 111–125.
24. Craig, H. Isotopic variations in meteoric waters. *Science* **1961**, *133*, 1702–1703.
25. Epstein, S.; Mayeda, T. Variation of ^{18}O content of waters from natural sources. *Geochem. Cosmochem. Acta* **1953**, *4*, 213–224.
26. Schmidt, A.; Santos, I.R.; Burnett, W.; Niencheski, F.; Knöller, K. Groundwater sources in a permeable coastal barrier: Evidence from stable isotopes. *J. Hydrol.* **2011**, *406*, 66–72.
27. Zektser, I.S.; Dzhamalov, R.G.; Everett, L.G. *Submarine Groundwater*; CRC Press: Boca Raton, FL, USA, 2007.
28. Gilli, E. Etudes des Sources Karstiques Sous-Marines et Littorales des Alpes Maritimes Entre Menton et Nice. In *Ministre de l' Environnement, Direction Régional de l'Environnement*; DREAL PACA: Marseille, France, 1997.
29. Mallast, U.; Siebert, C.; Gloaguen, R.; Friesen, J.; Rödiger, T.; Geyer, S.; Merz, R. How to identify groundwater-caused thermal anomalies in lakes based on multi-temporal satellite data in semi-arid regions. *Hydrol. Earth Syst. Sci.* **2013**, *10*, 4901–4949.
30. Gilli, E. Détection de sources sous-marines et précision de l'impluvium par mesure des variations de salinité. L'exemple de la source de Cabbé-Massolins (Roquebrune-Cap-Martin, France). *Comptes Rendus de l'Académie des Sciences–Series IIA–Earth Planet. Sci.* **1999**, *329*, 109–116.
31. Schubert, M.; Paschke, A.; Lieberman, E.; Burnett, W.C. Air-water partitioning of ^{222}Rn and its dependence on water salinity. *Environ. Sci. Technol.* **2012**, *46*, 3905–3911.
32. Moore, W.S.; Arnold, R. Measurement of ^{223}Ra and ^{224}Ra in coastal waters using a delayed coincidence counter. *J. Geophys. Res.* **1996**, *101*, 1321–1329.
33. Scholten, J.; Pham, M.K.; Blinova, O.; Charette, M.A.; Dulaiova, H.; Eriksson, M. Preparation of Mn-fiber standards for the efficiency calibration of the delayed coincidence counting system (RaDeCC). *Mar. Chem.* **2010**, *121*, 206–214.

34. Gehre, M.; Geilmann, H.; Richter, J.; Werner, R.A.; Brand, W.A. Continuous flow $^{2}H/^{1}H$ and $^{18}O/^{16}O$ analysis of water samples with dual inlet precision. *Rapid Commun. Mass Spectrom.* **2004**, *18*, 2650–2660.
35. Barsi, J.A.; Barker, J.L.; Schott, J.R. An Atmospheric Correction Parameter Calculator for a Single Thermal Band Earth-Sensing Instrument. In Proceedings of IGARSS03, Centre de Congres Pierre Baudis, Toulouse, France, 21–25 July 2003.
36. Johnson, A.G.; Glenn, C.R.; Burnett, W.C.; Peterson, R.N.; Lucey, P.G. Aerial infrared imaging reveals large nutrient-rich groundwater inputs to the ocean. *Geophys. Res. Lett.* **2008**, *35*, L15606.
37. Tsabaris, C.; Scholten, J.; Karageorgis, A.P.; Comanducci, J.F.; Georgopoulos, D.; Wee Kwong, L.L.; Patiris, D.L.; Papathanassiou, E. Underwater *in situ* measurements of radionuclides in selected submarine groundwater springs, Mediterranean Sea. *Radiat. Protect. Dosim.* **2010**, *142*, 273–281.
38. Ferrarin, C.; Rapaglia, J.; Zaggia, L.; Umgiesser, G.; Zuppi, G.M. Coincident application of a mass balance of radium and a hydrodynamic model for the seasonal quantification of groundwater flux into the Venice Lagoon, Italy. *Mar. Chem.* **2008**, *112*, 179–188.
39. Garcia-Solsona, E.; Garcia-Orellana, J.; Masque, P.; Rodellas, V.; Mejias, M.; Ballesteros, B.; Dominguez, J.A. Groundwater and nutrient discharge through karstic coastal springs (Castello, Spain). *Biogeosciences* **2010**, *7*, 2625–2638.
40. Rapaglia, J.; Koukoulas, S.; Zaggia, L.; Lichter, M.; Manfé, G.; Vafeidis, A.T. Quantification of submarine groundwater discharge and optimal radium sampling distribution in the Lesina Lagoon, Italy. *J. Mar. Syst.* **2012**, *91*, 11–19.
41. Gonneea, M.E.; Morris, P.J.; Dulaiova, H.; Charette, M.A. New perspectives on radium behavior within a subterranean estuary. *Mar. Chem.* **2008**, *109*, 250–267.
42. IAEA/WMO. Global Network of Isotopes in Precipitation. The GNIP Database 2014. Available online: http://www.iaea.org/water (accessed on 26 February 2014).